Inorganic Chemistry

Article

pubs.acs.org/IC

The $(N_4C_2)^{2-}$ Donor Set as Promising Motif for Bis(tridentate) Iron(II) Photoactive Compounds

Isabelle M. Dixon,* Fabienne Alary, Martial Boggio-Pasqua, and Jean-Louis Heully

Laboratoire de Chimie et Physique Quantiques, UMR 5626, CNRS/Université Paul Sabatier-Toulouse III, 118 route de Narbonne, Toulouse, France

Supporting Information

ABSTRACT: The ground and excited states of iron(II) bis(dipyridylbenzene) were probed by means of DFT and TDDFT. In comparison to the well-known $Fe(tpy)_2^{2+}$, this neutral complex should not suffer from ligand loss, and it displays a better absorption profile in the visible region. The relative energies of the spectroscopically relevant excited states (^{3}MLCT, ^{3}MC, ^{5}MLCT, and ^{5}MC) are quite different from those of its archetypical counterpart and thus make it a promising candidate for photophysics in general.

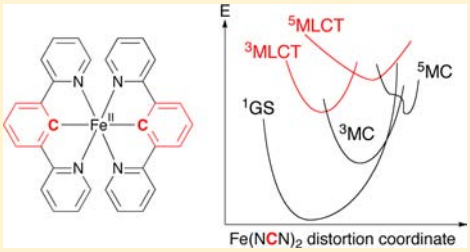

The abundance and low toxicity of iron with respect to ruthenium would certainly make it inescapable for photophysical applications if one could circumvent the kinetic lability of its polypyridine complexes. Iron(II) bis(terpyridine) ($Fe(tpy)_2^{2+}$) is indeed characterized by low-energy metal-centered excited states (or ligand-field states) that give rise to thermally labile ligands and prevent, for instance, the isolation of heteroleptic compounds. Iron(II) compounds of the $[FeN_6]^{2+}$ type have been thoroughly studied for spin crossover since the early 1980s,[1] and time-resolved spectroscopic studies have shown that a ^{5}MC state is populated in less than 700 fs from the initial singlet metal-to-ligand charge transfer (MLCT) state.[2] More recent studies on $Fe(bpy)_3^{2+}$ propose, following population of the ^{1}MLCT state, a first intersystem crossing (ISC) to the ^{3}MLCT state followed by ISC to the ^{5}MC state,[3] without involving an intermediate ^{3}MC state.[2,3] Destabilizing these MC states should thus render the MLCT states more usable, e.g. for electron transfer, and above all avoid ligand loss. The destabilization of MC states has been accomplished on ruthenium bis(terdentate)[4−10] or tris(bidentate)[11−18] polypyridine complexes by introducing one strongly σ donating cyclometalating ligand in place of a pyridine nitrogen in the first coordination sphere, which results in an increased splitting between the t_{2g}-like and e_g-like orbitals. Surprisingly, to the best of our knowledge, no publication has ever reported on cyclometalated iron compounds. Photophysical studies of carbon-containing iron(II) polypyridine compounds are in fact very limited. Logically, cyano complexes have been studied first. $Fe(bpy)_2(CN)_2$[19] and $Fe(bpy)(CN)_4^{2-}$[20] bear low-lying ligand field excited states. For the latter, only under very specific experimental conditions (namely solvent) can the ^{3}MLCT state be stabilized enough to be observed.[20] Nevertheless, the absence of long-lived excited states in solution does not preclude applications at an interface, such as sensitization of TiO_2 for solar cells, in which charge injection to the semiconductor is ultrafast[21] (<50 fs) and is able to compete with other deactivation mechanisms. Ferrere and Gregg indeed reported the first sensitization of TiO_2 by the tetracarboxylate derivative of $Fe(bpy)_2(CN)_2$.[22] However, this complex contains two monodentate ligands, which could compromise the long-term stability of the complex.[9] Recent DFT calculations have rationalized the observation that electron transfer to TiO_2 is 5 times more efficient on excitation in the higher energy MLCT band in comparison to that in the lower energy MLCT band, due to a better orientation of the orbital receiving the excited electron.[23] Similarly, the potential of $Fe(bpy)(CN)_4^{2-}$ as TiO_2 photosensitizer has been studied.[24] This complex can directly bind to TiO_2 via the cyanide nitrogen and is able to sensitize TiO_2 through two complementary mechanisms: direct metal-to-particle charge transfer (MPCT)[25] and more classical electron transfer from the bpy-based anion radical of the photopopulated ^{3}MLCT state. Very recently, Sundström and Wärnmark have reported a tetracarbene $[FeN_2C_4]^{2+}$ complex bearing a long-lived ^{3}MLCT state (τ = 9 ps; i.e. 2 orders of magnitude larger than for $Fe(tpy)_2^{2+}$).[26] The present work was therefore intended to probe by quantum methods the photophysical potential of a bis(cyclometalated) FeN_4C_2 polypyridine complex. 1,3-Di-2-pyridylbenzene (NCN)[27] was selected as ligand for its stronger ligand field in comparison to that of tpy, as well as for the "covalent" M−C bond it provides. It also maintains an axial symmetry, thus permitting directional electron transfer along this axis, for instance. The use of two NCN ligands provides neutral compounds with divalent metal ions, which can be advantageous for practical reasons (Figure 1).

METHODS

All calculations were performed with ORCA version 2.8 (rev 2360).[48] No pseudopotential was used on iron, given the conclusions recently

Received: June 28, 2013
Published: November 18, 2013

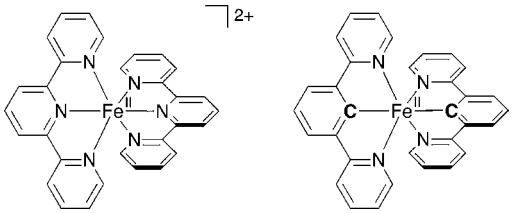

Figure 1. Chemical structures of $Fe(tpy)_2^{2+}$ and $Fe(NCN)_2$.

drawn by Truhlar and Xu.[49] Scalar relativistic effects were considered using ZORA.[50] The ZORA-adapted triple-ζ and polarized def2-TZVP(-f) basis set was used for all atoms.[51] Results with TZVP were qualitatively very similar. The B3LYP* hybrid functional was selected for this study (see computational details in the Supporting Information).[52] An empirical dispersion correction (VDW06) was also used to improve the geometries.[53] No symmetry constraints were applied, thus taking possible Jahn–Teller effects into consideration. Vibrations were calculated at the same level of theory following geometry optimizations, to ascertain the nature of the states as true minima (no imaginary frequency). The Mulliken spin density on the metal was used to indicate the nature of the excited states, and we also checked that their spin contamination was low. Natural orbitals,[54] obtained by diagonalization of the density matrix, are intrinsically more localized than the canonical Kohn–Sham molecular orbitals. As such, they constitute a convenient way to picture open-shell wave functions and have been used throughout this study for triplet and quintet states. Given that the X-ray geometry of $Fe(tpy)_2^{2+}$ is best reproduced by the PBE0 functional, the TDDFT calculations were performed at the PBE0-optimized ground state geometries, in contrast to a recent study which analyzed various combinations of functionals for geometry optimization and TDDFT.[55] An asymptotic correction[56] was applied, following the determination of ionization potentials. Solvent was included as a continuum with COSMO, and 40 roots were computed. The absorption spectra were generated by the ASA[57] module of ORCA using Gaussians, with a midheight width of 1766 cm^{-1}.

RESULTS

In recent years, the sophistication of quantum chemistry codes and methods and the increase in computational power have facilitated the exploration of excited state potential energy surfaces. Recently, a few detailed DFT studies interested in describing several different excited states of ruthenium complexes and their possible deactivation pathways have appeared in the literature.[28−40] The powerful predictive character of such studies is progressively being recognized. Although not routine at all, this type of complex calculation is gradually taking an increasing importance in the full research process, sometimes coming before/without any experimental data. Focusing on the design of molecules bearing specific physical properties, some remarkable examples have been reported in the fields of spin crossover,[41] two-photon absorption,[42] organic[43,44] and inorganic[45] photovoltaics, optimization of the spectral properties of chromophores,[46,47] and anticipation of the photophysical properties of novel complexes (refs 32 and 38 and this work). The first part of this study has thus been devoted to the validation of our method by reproducing the available experimental data on $Fe(tpy)_2^{2+}$.

The bis(terpyridine) Complex $Fe(tpy)_2^{2+}$. The experimental data on $Fe(tpy)_2^{2+}$ includes the ground-state structure,[58,59] absorption properties,[60,61] oxidation potential,[62] nature[2,62] and lifetime[62−64] of the photopopulated ^{5}MC excited state, and structural and electronic data on the ^{5}MC excited state by transient X-ray absorption spectroscopy.[65] The available computational data on this complex concern DFT ground-state optimization and UV–vis absorption modeling,[65,66] as well as exploration of the quintet MC excited state by DFT[67] and very recently of the triplet and quintet MC excited states by TD-DFT and CASPT2 methods.[68] The results reported here both reinforce the previous data and allow a full description of the excited states, particularly in terms of orbitals (Figure S1, Supporting Information). In line with the experimental data, all of the lowest optimized excited states have MC character. The major geometrical variations among ground (singlet), triplet, and quintet states are a marked elongation of the Fe–N bonds and a subsequent gradual closing of the NFeN bite angle (Table S1 and Figure S9, Supporting Information). Remarkably, there are different types of MC states, a fact that had not been pointed out in previous reports: the interaction between the singly occupied e_g orbital(s) and the bound nitrogen atoms is overall *nonbonding* for the ^{3}MC state, while it is clearly *antibonding* in the ^{5}MC state (Figure 2). In addition, this antibonding interaction

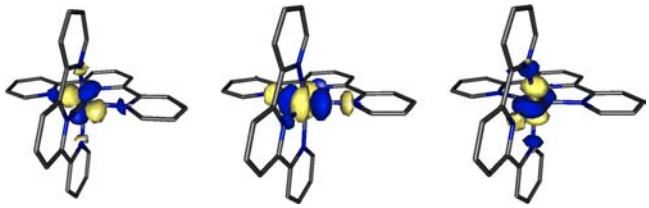

Figure 2. Natural orbitals receiving the excited electron in the ^{3}MC state (left) and in the ^{5}MC state (center and right) of $Fe(tpy)_2^{2+}$. The Fe–N interactions are overall nonbonding in the ^{3}MC state and antibonding in the ^{5}MC state.

involves the three nitrogen atoms of the same tpy ligand, which explains the spontaneous ligand decoordination specifically observed in the ^{5}MC state. The occupation of the orbitals shown in Figure 2 is responsible for the geometrical distortions of the metal-centered excited states.

The bis(cyclometalated) Complex $Fe(NCN)_2$. *Ground State Orbitals.* To highlight the specificities of the bis(dipyridylbenzene) complex $Fe(NCN)_2$, a close examination of the ground-state orbitals is first undertaken. Indeed, among these ground-state orbitals, the t_{2g} orbitals are HOMO, HOMO-1, and HOMO-2, with a small contribution from the phenyl rings in HOMO and HOMO-1. Covalent Fe–C σ bonds are found in HOMO-3 and HOMO-8, and a metal–phenyl π-bonding interaction is found in HOMO-6 and HOMO-7 (Figure 3). The virtual LUMO+8 is similar to LUMO+8 of $Fe(tpy)_2^{2+}$, with antibonding interactions with the four peripheral N atoms (Figure S4, Supporting Information). However, as elongating a covalent Fe–C bond costs far more energy than elongating a dative Fe–N bond, the tendency to form MC states will not be as strong.

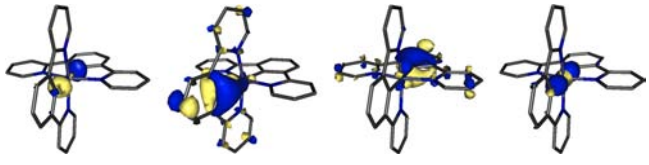

Figure 3. Kohn–Sham orbitals of the ground state of $Fe(NCN)_2$ displaying strong contributions from the bound carbon atoms. From left to right: HOMO-3, HOMO-6, HOMO-7, and HOMO-8.

dx.doi.org/10.1021/ic402453p | Inorg. Chem. 2013, 52, 13369−13374

Absorption Spectrum. Time-dependent DFT was used to probe the absorption properties of the complexes. After reproducing the experimental absorption of $Fe(tpy)_2^{2+}$,[60,61] the same conditions were applied to model the absorption of $Fe(NCN)_2$: the lowest energy band was shifted from 537 to 614 nm upon bis(cyclometalation) (Tables S5−S7 and Figures S13−S15, Supporting Information). Therefore, the introduction of two carbon atoms in the Fe(II) coordination sphere results in a pronounced bathochromic shift of the spectrum, together with a relatively strong absorption extending beyond 650 nm (Figure 4). Bathochromicity and hyperchromicity are

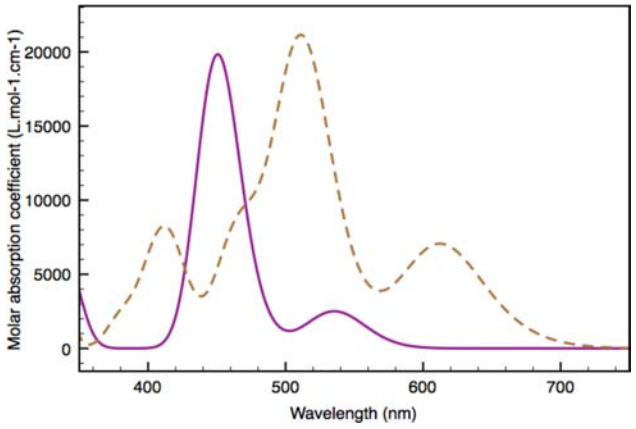

Figure 4. Computed UV−vis absorption spectra of $Fe(tpy)_2^{2+}$ (solid line) and $Fe(NCN)_2$ (dotted line) in water in the 350−750 nm range.

favorable in view of using such compounds as dyes: e.g., for solar cells. A further bathochromic shift of the absorption can be expected after appropriate substitution of selected rings and a further red shift upon adsorption on TiO_2.[69] Solvent effects can also be invoked to further stabilize the CT states, as shown for $Fe(bpy)(CN)_4^{2-}$ in acetone.[20]

Excited States. At odds with $Fe(tpy)_2^{2+}$, four different excited states were identified as true minima for $Fe(NCN)_2$: ^{3}MLCT, ^{3}MC, ^{5}MLCT, and ^{5}MC. The Fe−N bond length increases from 2.00 Å in the ground state and in the ^{3}MLCT state[70] to 2.16 Å in the ^{3}MC state and 2.30 Å in the ^{5}MC state (Table S2, Supporting Information). Similarly, the Fe−C bond length increases from 1.90 Å (^{1}GS) to 1.92 Å (^{3}MLCT and ^{3}MC states) and to 2.08 Å in the ^{5}MC state. The relatively limited elongation of the Fe−C distance is related to the covalent nature of these bonds, which is responsible for the strong destabilization of the ^{5}MC state. A strong distortion of the complex, in which the C−Fe−C angle drops from 180 to 167° (Figure S10, Supporting Information), is observed in the ^{5}MC state and helps to avoid Fe−C antibonding interactions. It is noteworthy that, unlike the case for $Fe(tpy)_2^{2+}$, ligand labilization is not expected to occur in this ^{5}MC state since the interactions are *antibonding* with two nitrogen atoms but *bonding* with two carbon atoms (Figure 5): therefore, the ligands are repelled but are nevertheless held firmly by the covalent Fe−C bonds. In the lowest ^{5}MC state, the five d orbitals spread over 2.1 eV, which is twice the value for $Fe(tpy)_2^{2+}$. This situation should disfavor the emergence of magnetic properties in bis(cyclometalated) Fe(II) compounds. The ^{5}MLCT state, which bears three unpaired electrons on the metal and one on the ligand, displays a distorted geometry (see inset of Figure 7 and Table S2 (Supporting Information)). The

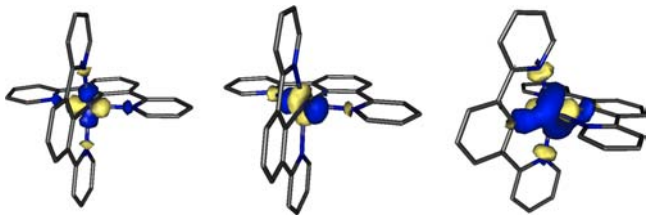

Figure 5. Natural orbitals receiving the excited electron in the ^{3}MC state (left) and in the ^{5}MC state (center and right) of $Fe(NCN)_2$. The ^{3}MC state involves four Fe−N antibonding interactions, while the ^{5}MC state involves two Fe−N antibonding interactions (center and right) and two Fe−C bonding interactions (right). On the right, the yellow lobes on the metal do not point toward the carbon atoms.

ligand receiving the electron is overall much less repelled than the other, resulting in Fe−N bond lengths of 2.07 and 2.19 Å, respectively. This quintet state, which can be seen as the superimposition of ^{3}MC and ^{3}MLCT states, can in fact be expected to combine both characters and physical properties; hence, a longer but more explicit acronym could be more appropriate (e.g., ^{5}MC-MLCT). The only other theoretical description of such a ^{5}MLCT state in a Fe(II) compound is an ab initio CASPT2 study,[71] which is far more computationally demanding.

Minimum Energy Crossing Points. The optimization of minimum energy crossing points (MECPs) between potential energy surfaces of different spin multiplicity yields information regarding the ease of a state to undergo intersystem crossing, in terms of both energetic cost and geometrical changes (Tables S3 and S4, Supporting Information). This type of study is compulsory when one wants to envisage possible deactivation pathways of a photopopulated excited state. In this work, we have focused on MECPs that are relevant to the deactivation of the ^{5}MC state (Figure 6). All of them involve relatively low

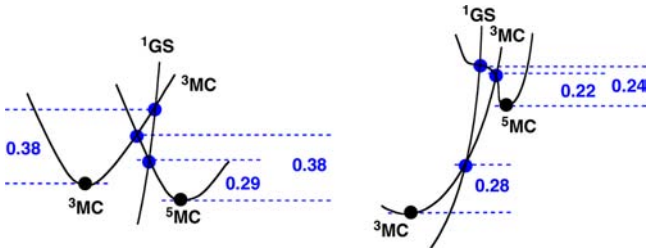

Figure 6. MECPs (in blue) of $Fe(tpy)_2^{2+}$ (left) and $Fe(NCN)_2$ (right) and energy gaps in eV.

activation energies, ranging between 5 and 9 kcal/mol (21−37 kJ/mol). In the case of $Fe(tpy)_2^{2+}$, a direct ^{5}MC/^{1}GS crossing would imply overcoming a 0.29 eV barrier (and shortening the $Fe-N_{periph}$ bonds by 0.04 Å). An alternative two-step mechanism, via the ^{3}MC state, can be envisaged. In this case, the ^{5}MC/^{3}MC crossing involves a 0.38 eV barrier (and a 0.03 Å shrinkage) and is followed by a ^{3}MC/^{1}GS crossing, also involving a 0.38 eV barrier (and the removal of one tpy, with 0.07 and 0.20 Å elongations of the corresponding $Fe-N_{periph}$ bonds). For $Fe(NCN)_2$, reaching the ^{5}MC/^{3}MC crossing point from the ^{5}MC minimum only costs 0.22 eV (0.01 Å shrinkage), which is comparable in terms of energy to the cost of the ^{5}MC/^{1}GS crossing (0.24 eV but 0.05 Å shrinkage). The second part of the two-step mechanism, i.e. reaching the ^{3}MC/^{1}GS crossing from the ^{3}MC minimum, involves overcoming a 0.28

dx.doi.org/10.1021/ic402453p | *Inorg. Chem.* 2013, 52, 13369−13374

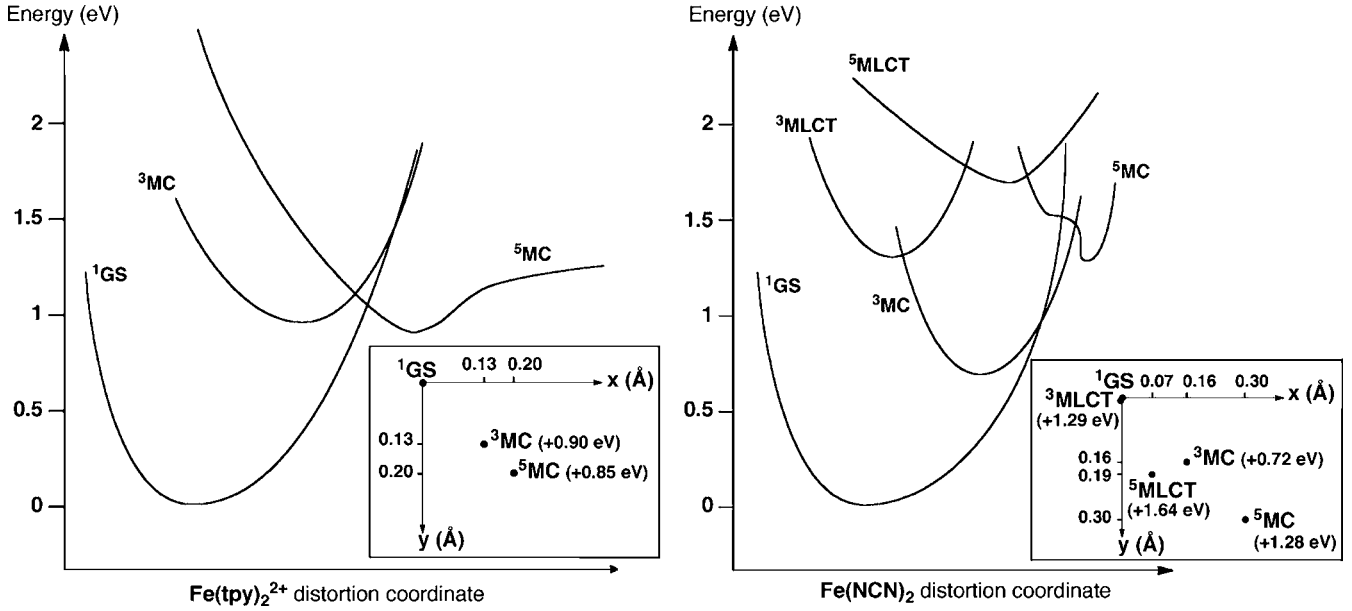

Figure 7. Potential energy curves versus a multidimensional distortion coordinate. The insets show the schematic projection of the minima on the plane defined by the Fe−N_{periph} stretch for one ligand (x) and the other (y). In this representation, MC states lie on the diagonal while the ^{5}MLCT state does not. Energy gaps with ^{1}GS are given in parentheses.

eV barrier (and a 0.06 Å elongation). One can note that the activation energies are always lower for $Fe(NCN)_2$ than for $Fe(tpy)_2^{2+}$.

DISCUSSION

Figure 7 displays schematic potential energy curves for the various states of $Fe(tpy)_2^{2+}$ and $Fe(NCN)_2$, versus a multidimensional distortion coordinate that connects the ground state and the ^{5}MC state. It is noteworthy that the left half of Figure 7 is qualitatively very similar to the CASPT2 potential energy curves reported for $Fe(tpy)_2^{2+}$,[68] strengthening our confidence in the predictive character of this DFT study. Overall, the introduction of two carbon atoms in the Fe coordination sphere restores accessible ^{3}MLCT and ^{5}MLCT minima and strongly destabilizes the ^{5}MC state with respect to the ground state, as expected with strongly σ donating ligands.[72] Nevertheless, the charge-transfer states can be expected to be short-lived, due to the presence of more stable ligand-field states. Qualitatively, given the relative positions of minima and MECPs, the mechanism and efficiency for the population and depopulation of the ^{5}MC state can be expected to be truly different from those of $Fe(tpy)_2^{2+}$. It is particularly striking from Figures 6 and 7 that the lifetime of the ^{5}MC state can be expected to be shorter for $Fe(NCN)_2$ than for $Fe(tpy)_2^{2+}$, given the inevitable ^{5}MC−^{3}MC−GS cascade with two carbon atoms. In addition, the ^{5}MC state is most probably exclusively populated from the ^{5}MLCT state, itself being populated from another upper-lying MLCT state (not shown on Figure 7). One could speculate, with a particular excitation wavelength/setup, to favor the ^{1}MLCT−^{3}MLCT−^{3}MC−^{1}GS route, while another excitation wavelength/setup could favor a ^{1}MLCT′−^{3}MLCT′−^{5}MLCT−^{5}MC−^{3}MC−^{1}GS route. The ^{3}MLCT state could deactivate either by near-IR emission or by population of the ^{3}MC state, which in turn can populate the ^{1}GS.

CONCLUSION

To summarize, bis(cyclometalated) Fe(II) polypyridine complexes seem promising compounds for photophysics, allowing us to circumvent the two major drawbacks of $Fe(tpy)_2^{2+}$: (i) no tendency toward thermal or photochemical ligand loss is expected due to the anchorage of the ligands via covalent Fe−C bonds; (ii) in comparison to $Fe(tpy)_2^{2+}$, the ^{5}MC state of $Fe(NCN)_2$ does not appear as a trap with potentially long lifetime and should not kill the photophysical properties of these compounds, particularly electron transfer. $Fe(NCN)_2$ thus paves the way toward a new family of kinetically stable Fe(II) compounds, allowing real chemistry and physics to be envisaged: e.g., adjustment of their properties with substituents, solvent, temperature etc. In order to dispose of potentially luminescent MLCT states with longer lifetimes, it is crucial to consider the position of the carbon atoms: when placed on the central cycles of the tridentate ligand, facing each other, they do not prevent the population of an MC state that elongates the four peripheral Fe−N bonds. To recover a measurable luminescence, it is desirable to feature ligand-field states that involve at least one antibonding Fe−C interaction, which would automatically destabilize the MC states by a significant amount of energy. We are therefore currently exploring the excited states of all isomers of $Fe(NCN)_2$ to rationalize the energies of the excited states with respect to the position of the carbon atoms, in a "molecular design" approach. Similarly, we are currently transposing this study to Ru(II) analogues.

ASSOCIATED CONTENT

Supporting Information

Text, figures, and tables giving computational details, selected geometric parameters and orbitals, major angular variations as a function of electronic configuration, energy gaps among singlets, triplets, and quintets, MECP energies and geometries, TDDFT modeling of absorption maxima and orbital analysis, and Cartesian coordinates of all minima (and their absolute

dx.doi.org/10.1021/ic402453p | Inorg. Chem. 2013, 52, 13369−13374

energies) for $Fe(tpy)_2^{2+}$ and $Fe(NCN)_2$. This material is available free of charge via the Internet at http://pubs.acs.org.

AUTHOR INFORMATION

Corresponding Author

*E-mail for I.M.D.: isabelle.dixon@irsamc.ups-tlse.fr.

Notes

The authors declare no competing financial interest.

ACKNOWLEDGMENTS

This work was performed using HPC resources from CALMIP (Grant 2012-p1112). G. Rapenne is also acknowledged for his comments on the paper.

REFERENCES

(1) Gütlich, P.; Hauser, A. *Coord. Chem. Rev.* **1990**, *97*, 1 and references therein.

(2) McCusker, J. K.; Walda, K. N.; Dunn, R. C.; Simon, J. D.; Magde, D.; Hendrickson, D. N. *J. Am. Chem. Soc.* **1993**, *115*, 298.

(3) (a) Gawelda, W.; Pham, V.-T.; Benfatto, M.; Zaushitsyn, Y.; Kaiser, M.; Grolimund, D.; Johnson, S. L.; Abela, R.; Hauser, A.; Bressler, C.; Chergui, M. *Phys. Rev. Lett.* **2007**, *98*, 057401. (b) Cannizzo, A.; Milne, C. J.; Consani, C.; Gawelda, W.; Bressler, C.; van Mourik, F.; Chergui, M. *Coord. Chem. Rev.* **2010**, *254*, 2677 and references therein. (c) Chergui, M., Ultrafast studies of the light-induced spin change in Fe(II)-polypyridine complexes. In *Spin-Crossover Materials: Properties and Applications*; Halcrow, M. A., Ed.; Wiley: Hoboken, NJ, 2013; pp 405−424.

(4) Wadman, S. H.; Kroon, J. M.; Bakker, K.; Lutz, M.; Spek, A. L.; van Klink, G. P. M.; van Koten, G. *Chem. Commun.* **2007**, 1907.

(5) Wadman, S. H.; Lutz, M.; Tooke, D. M.; Spek, A. L.; Hartl, F.; Havenith, R. W. A.; van Klink, G. P. M.; van Koten, G. *Inorg. Chem.* **2009**, *48*, 1887.

(6) Jäger, M.; Smeigh, A.; Lombeck, F.; Görls, H.; Collin, J.-P.; Sauvage, J.-P.; Hammarström, L.; Johansson, O. *Inorg. Chem.* **2010**, *49*, 374.

(7) Kim, J.-J.; Choi, H.; Paek, S.; Kim, C.; Lim, K.; Ju, M.-J.; Kang, H. S.; Kang, M.-S.; Ko, J. *Inorg. Chem.* **2011**, *50*, 11340.

(8) Kisserwan, H.; Kamar, A.; Shoker, T.; Ghaddar, T. H. *Dalton Trans.* **2012**, *41*, 10643.

(9) Bomben, P. G.; Robson, K. C. D.; Koivisto, B. D.; Berlinguette, C. P. *Coord. Chem. Rev.* **2012**, *256*, 1438 and references therein..

(10) Robson, K. C. D.; Bomben, P. G.; Berlinguette, C. P. *Dalton Trans.* **2012**, *41*, 7814 and references therein.

(11) Li, E. Y.; Cheng, Y.-M.; Hsu, C.-C.; Chou, P.-T.; Lee, G.-H.; Lin, I.-H.; Chi, Y.; Liu, C.-S. *Inorg. Chem.* **2006**, *45*, 8041.

(12) Bessho, T.; Yoneda, E.; Yum, J.-H.; Guglielmi, M.; Tavernelli, I.; Imai, H.; Rothlisberger, U.; Nazeeruddin, Md. K.; Grätzel, M. *J. Am. Chem. Soc.* **2009**, *131*, 5930.

(13) Padhi, S. K.; Tanaka, K. *Inorg. Chem.* **2011**, *50*, 10718.

(14) Abbotto, A.; Coluccini, C.; Dell'Orto, E.; Manfredi, N.; Trifiletti, V.; Salamone, M. M.; Ruffo, R.; Acciarri, M.; Colombo, A.; Dragonetti, C.; Ordanini, S.; Roberto, D.; Valore, A. *Dalton Trans.* **2012**, *41*, 11731.

(15) Muro-Small, M. L.; Yarnell, J. E.; McCusker, C. E.; Castellano, F. N. *Eur. J. Inorg. Chem.* **2012**, 4004.

(16) Ji, Z.; Natu, G.; Huang, Z.; Kokhan, O.; Zhang, X.; Wu, Y. *J. Phys. Chem. C* **2012**, *116*, 16854.

(17) Peña, B.; Leed, N. A.; Dunbar, K. R.; Turro, C. *J. Phys. Chem. C* **2012**, *116*, 22186.

(18) Pogozhev, D. V.; Bezdek, M. J.; Schauer, P. A.; Berlinguette, C. P. *Inorg. Chem.* **2013**, *52*, 3001. See also refs 9 and 10.

(19) Winkler, J. R.; Sutin, N. *Inorg. Chem.* **1987**, *26*, 220.

(20) Winkler, J. R.; Creutz, C.; Sutin, N. *J. Am. Chem. Soc.* **1987**, *109*, 3470.

(21) For the Ru-based N_3 dye: (a) Ellingson, R. J.; Asbury, J. B.; Ferrere, S.; Ghosh, H. N.; Sprague, J. R.; Lian, T. Q.; Nozik, A. J. *J. Phys. Chem. B* **1998**, *102*, 6455. For $Fe(CN)_6^{4-}$: (b) Ghosh, H. N.; Asbury, J. B.; Lian, T. Q. *J. Phys. Chem. B* **1998**, *102*, 6482.

(22) Ferrere, S.; Gregg, B. A. *J. Am. Chem. Soc.* **1998**, *120*, 843.

(23) Bowman, D. N.; Blew, J. H.; Tsuchiya, T.; Jakubikova, E. *Inorg. Chem.* **2013**, *52*, 8621.

(24) (a) Yang, M.; Thompson, D. W.; Meyer, G. J. *Inorg. Chem.* **2000**, *39*, 3738. (b) Yang, M.; Thompson, D. W.; Meyer, G. J. *Inorg. Chem.* **2002**, *41*, 1254.

(25) Ardo, S.; Meyer, G. J. *Chem. Soc. Rev.* **2009**, *38*, 115.

(26) Liu, Y.; Harlang, T.; Canton, S. E.; Chábera, P.; Suárez-Alcántara, K.; Fleckhaus, A.; Vithanage, D. A.; Göransson, E.; Corani, A.; Lomoth, R.; Sundström, V.; Wärnmark, K. *Chem. Commun.* **2013**, *49*, 6412.

(27) Williams, J. A. G. *Chem. Soc. Rev.* **2009**, *38*, 1783 and references therein.

(28) Alary, F.; Boggio-Pasqua, M.; Heully, J.-L.; Marsden, C. J.; Vicendo, P. *Inorg. Chem.* **2008**, *47*, 5259.

(29) Borg, O. A.; Godinho, S. S. M. C.; Lundqvist, M. J.; Lunell, S.; Persson, P. *J. Phys. Chem. A* **2008**, *112*, 4470.

(30) Heully, J.-L.; Alary, F.; Boggio-Pasqua, M. *J. Chem. Phys.* **2009**, *131*, 184308.

(31) Dixon, I. M.; Alary, F.; Heully, J.-L. *Dalton Trans.* **2010**, *39*, 10959.

(32) Guillon, T.; Boggio-Pasqua, M.; Alary, F.; Heully, J.-L.; Lebon, E.; Sutra, P.; Igau, A. *Inorg. Chem.* **2010**, *49*, 8862.

(33) Göttle, A. J.; Dixon, I. M.; Alary, F.; Heully, J.-L.; Boggio-Pasqua, M. *J. Am. Chem. Soc.* **2011**, *133*, 9172.

(34) Welby, C. E.; Grkinic, S.; Zahid, A.; Uppal, B. S.; Gibson, E. A.; Rice, C. R.; Elliott, P. I. P. *Dalton Trans.* **2012**, *41*, 7637.

(35) Lebon, E.; Bastin, S.; Sutra, P.; Vendier, L.; Piau, R. E.; Dixon, I. M.; Boggio-Pasqua, M.; Alary, F.; Heully, J.-L.; Igau, A.; Juris, A. *Chem. Commun.* **2012**, *48*, 741.

(36) (a) Österman, T.; Abrahamsson, M.; Becker, H.-C.; Hammarström, L.; Persson, P. *J. Phys. Chem. A* **2012**, *116*, 1041. (b) Österman, T.; Persson, P. *Chem. Phys.* **2012**, *407*, 76.

(37) Piau, R. E.; Guillon, T.; Lebon, E.; Perrot, N.; Alary, F.; Boggio-Pasqua, M.; Heully, J.-L.; Juris, A.; Sutra, P.; Igau, A. *New J. Chem.* **2012**, *36*, 2484.

(38) Vieuxmaire, O. P. J.; Piau, R. E.; Alary, F.; Heully, J.-L.; Sutra, P.; Igau, A.; Boggio-Pasqua, M. *J. Phys. Chem. A* Accepted for publication. 10.1021/jp408898n.

(39) Vallett, P. J.; Damrauer, N. H. *J. Phys. Chem. A* **2013**, *117*, 6489.

(40) Breivogel, A.; Meister, M.; Förster, C.; Laquai, F.; Heinze, K. *Chem. Eur. J.* **2013**, *19*, 13745.

(41) Deeth, R. J.; Anastasi, A. E.; Wilcockson, M. J. *J. Am. Chem. Soc.* **2010**, *132*, 6876.

(42) Chattopadhyaya, M.; Alam, Md. M.; Chakrabarti, S. *J. Phys. Chem. A* **2011**, *115*, 2607.

(43) Hachmann, J.; Olivares-Amaya, R.; Atahan-Evrenk, S.; Amador-Bedolla, C.; Sánchez-Carrera, R. S.; Gold-Parker, A.; Vogt, L.; Brockway, A. M.; Aspuru-Guzik, A. *J. Phys. Chem. Lett.* **2012**, *2*, 2241.

(44) Agrawal, S.; English, N. J.; Thampi, K. R.; MacElroy, J. M. D. *Phys. Chem. Chem. Phys.* **2012**, *14*, 12044.

(45) Labat, F.; Le Bahers, T.; Ciofini, I.; Adamo, C. *Acc. Chem. Res.* **2012**, *45*, 1268.

(46) Chica, R. A.; Moore, M. M.; Allen, B. D.; Mayo, S. L. *Proc. Natl. Acad. Sci. U.S.A.* **2010**, *107*, 20257.

(47) Prampolini, G.; Bellina, F.; Biczysko, M.; Cappelli, C.; Carta, L.; Lessi, M.; Pucci, A.; Ruggeri, G.; Barone, V. *Chem. Eur. J.* **2013**, *19*, 1996.

(48) Neese, F.; Becker, U.; Ganyushin, D.; Liakos, D.; Kossmann, S.; Petrenko, T.; Riplinger, C.; Wennmohs, F. *ORCA version 2.8, an ab initio, density functional and semiempirical program package*; Universität Bonn, Bonn, Germany, 2009.

(49) Xu, X.; Truhlar, D. G. *J. Chem. Theory Comput.* **2012**, *8*, 80.

(50) van Wüllen, C. *J. Chem. Phys.* **1998**, *109*, 392.

(51) Pantazis, D. A.; Chen, X. Y.; Landis, C. R.; Neese, F. *J. Chem. Theory Comput.* **2008**, *4*, 908.

(52) (a) Reiher, M.; Salomon, O.; Hess, B. A. *Theor. Chem. Acc.* **2001**, *107*, 48. (b) Reiher, M. *Inorg. Chem.* **2002**, *41*, 6928.
(53) Grimme, S. *J. Comput. Chem.* **2006**, *27*, 1787−1799.
(54) Weinhold, F.; Landis, C. R. *Chem. Educ.: Res. Pract. Eur.* **2001**, *2*, 91.
(55) Zanna, N.; Monari, A.; Assfeld, X. *J. Phys. Chem. A* **2012**, *116*, 11905.
(56) Grüning, M.; Gritsenko, O. V.; vanGisbergen, S. J. A.; Baerends, E. J. *J. Chem. Phys.* **2001**, *114*, 652.
(57) Petrenko, T.; Neese, F. *J. Chem. Phys.* **2007**, *127*, 164319.
(58) Baker, A. T.; Goodwin, H. A. *Aust. J. Chem.* **1985**, *38*, 207.
(59) Oshio, H.; Spiering, H.; Ksenofontov, V.; Renz, F.; Gütlich, P. *Inorg. Chem.* **2001**, *40*, 1143.
(60) Ford-Smith, H.; Sutin, N. *J. Am. Chem. Soc.* **1961**, *83*, 1830.
(61) Krumholz, P. *Inorg. Chem.* **1965**, *4*, 612.
(62) Creutz, C.; Chou, M.; Netzel, T. L.; Okumura, M.; Sutin, N. *J. Am. Chem. Soc.* **1980**, *102*, 1309.
(63) A slightly longer room temperature lifetime of 5.4 ns was estimated from measurements at 240 K: McCusker, J. K.; Rheingold, A. L.; Hendrickson, D. N. *Inorg. Chem.* **1996**, *35*, 2100.
(64) Renz, F.; Oshio, H.; Ksenofontov, V.; Waldeck, M.; Spiering, H.; Gütlich, P. *Angew. Chem., Int. Ed.* **2000**, *39*, 3699.
(65) Cho, H.; Strader, M. L.; Hong, K.; Jamula, L.; Gullikson, E. M.; Kim, T. K.; de Groot, F. M. F.; McCusker, J. K.; Schoenlein, R. W.; Huse, N. *Faraday Discuss.* **2012**, *157*, 463.
(66) Wadman, S. H.; van der Geer, E. P. L.; Havenith, R. W. A.; Klein Gebbink, R. J. M.; van Klink, G. P. M.; van Koten, G. *J. Organomet. Chem.* **2008**, *693*, 3188.
(67) Hauser, A.; Enachescu, C.; Lawson Daku, L. M.; Vargas, A.; Amstutz, N. *Coord. Chem. Rev.* **2006**, *250*, 1642.
(68) Papai, M.; Vanko, G.; de Graaf, C.; Rozgonyi, T. *J. Chem. Theory Comput.* **2013**, *9*, 509.
(69) Ferrere, S. *Chem. Mater.* **2000**, *12*, 1083.
(70) The relaxation coordinate linking the ground state and the ^{3}MLCT minimum involves C−C bond length variations rather than Fe−N elongations.
(71) de Graaf, C.; Sousa, C. *Int. J. Quantum Chem.* **2011**, *111*, 3385.
(72) The stronger NCN ligand field results in a larger ligand-field splitting: the d-block orbitals spread over 1.15 eV with the N_6 donor set but over 2.38 eV with the $(N_4C_2)^{2-}$ donor set.